BIOCHEMISTRY
including biophysical chemistry & molecular biology

Article

pubs.acs.org/biochemistry

Autoinhibition and Phosphorylation-Induced Activation of Phospholipase C-γ Isozymes

Nicole Hajicek,[†] Thomas H. Charpentier,[†] Jeremy R. Rush,[†,∥] T. Kendall Harden,[†] and John Sondek*[,†,‡]

[†]Department of Pharmacology and [‡]Department of Biochemistry and Biophysics and Lineberger Comprehensive Cancer Center, University of North Carolina School of Medicine, Chapel Hill, North Carolina 27599-7365, United States

ABSTRACT: Multiple extracellular stimuli, such as growth factors and antigens, initiate signaling cascades through tyrosine phosphorylation and activation of phospholipase C-γ (PLC-γ) isozymes. Like most other PLCs, PLC-γ1 is basally autoinhibited by its X−Y linker, which separates the X- and Y-boxes of the catalytic core. The C-terminal SH2 (cSH2) domain within the X−Y linker is the critical determinant for autoinhibition of phospholipase activity. Release of autoinhibition requires an intramolecular interaction between the cSH2 domain and a phosphorylated tyrosine, Tyr783, also located within the X−Y linker. The molecular mechanisms that mediate autoinhibition and phosphorylation-induced activation have not been defined. Here, we describe structures of the cSH2 domain both alone and bound to a PLC-γ1 peptide encompassing phosphorylated Tyr783. The cSH2 domain remains largely unaltered by peptide engagement. Point mutations in the cSH2 domain located at the interface with the peptide were sufficient to constitutively activate PLC-γ1, suggesting that peptide engagement directly interferes with the capacity of the cSH2 domain to block the lipase active site. This idea is supported by mutations in a complementary surface of the catalytic core that also enhanced phospholipase activity.

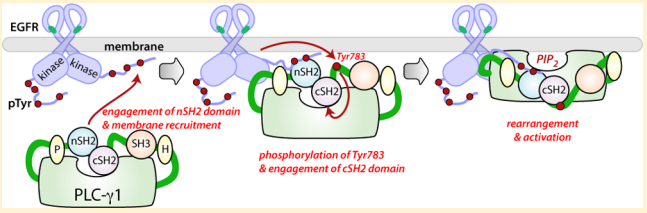

Diverse extracellular stimuli, including hormones, neurotransmitters, antigens, and growth factors, promote phospholipase C (PLC)-catalyzed hydrolysis of the minor membrane phospholipid phosphatidylinositol 4,5-bisphosphate [PtdIns(4,5)P_2] to generate the intracellular second messengers inositol 1,4,5-trisphosphate [Ins(1,4,5)P_3] and diacylglycerol.[1] Ins(1,4,5)P_3 and diacylglycerol mobilize intracellular calcium and activate PKC isozymes, respectively, to regulate multiple cellular processes, including fertilization, proliferation, differentiation, and chemotaxis.[2]

Six families of PLCs, PLC-β, -γ, -δ, -ε, -ζ, and -η, including 13 distinct isozymes, exist in humans.[1] With the exception of the sperm-specific isozyme PLC-ζ, PLCs have a common core architecture consisting of a pleckstrin homology (PH) domain, a series of EF hands, a catalytic triosephosphate isomerase (TIM) barrel split into X- and Y-boxes by a variable-length linker (X−Y linker), and a C2 domain. Most PLCs also contain additional domains, which engender isozyme-specific regulation. We have proposed a general model of regulation in which the X−Y linker basally autoinhibits PLC isozymes. In many PLCs, the X−Y linker is disordered and negatively charged, and its deletion accelerates phospholipase activity *in vitro* and in cells.[3] We posit that autoinhibition is due to electrostatic repulsion between the linker and membranes, as well as physical occlusion of the active site.[3−5] As a result of these observations, we proposed a model of interfacial activation in which PLCs are recruited to, and oriented at, membranes, leading to a concomitant displacement of the X−Y linker from the active site and enhanced phospholipase activity.

PLC-γ isozymes (PLC-γ1 and -γ2) uniquely possess a highly elaborated X−Y linker, which contains two Src homology 2 (SH2) domains, an SH3 domain, and a split PH domain, suggesting that these isozymes exhibit a distinct mode of regulation. Indeed, this domain architecture engenders PLC-γ-specific activation by multiple tyrosine kinases, and tyrosine phosphorylation within the X−Y linker stimulates the activity of PLC-γ isozymes *in vitro* and in cells.[6−9] In particular, phosphorylation of Tyr783 in PLC-γ1 is critical for activation downstream of receptor tyrosine kinases (RTKs) and immune cell receptors.[7,9,10] We recently demonstrated that PLC-γ isozymes are basally autoinhibited by the X−Y linker. Deletion of the C-terminal SH2 (cSH2) domain within the X−Y linker was sufficient to constitutively activate PLC-γ1. This activation was similar to deletion of the entire X−Y linker.[9] Therefore, the cSH2 domain represents the core element required for autoinhibition of lipase activity. Further deletion mapping defined 10 amino acids encompassing the BG loop and βG strand at the C-terminus of the cSH2 domain as critical for autoinhibitory capacity. We also demonstrated that activation of PLC-γ1 requires that the cSH2 domain engage phosphorylated Tyr783 and that this engagement results in an allosteric rearrangement of the linker coupled to activation. This allosteric rearrangement and activation is recapitulated by deletion of the BG loop and βG strand. Therefore, we postulate that PLC-γ1 couples tyrosine phosphorylation to conformational rearrangements within the X−Y linker that drive phospholipase activity.

Received: April 5, 2013
Revised: June 17, 2013
Published: June 18, 2013

   dx.doi.org/10.1021/bi400433b | *Biochemistry* 2013, 52, 4810−4819

While this model explains many aspects of the phosphorylation-dependent activation of the PLC-γ isozymes, several questions remain unresolved. For example, the mechanism by which elements within the cSH2 domain, specifically the BG loop and βG strand, contribute to the autoinhibition of PLC-γ1 activity is poorly understood. Here, we used a combination of structural biology and cell-based measures of phospholipase activity to propose that PLC-γ isozymes are regulated by direct competition of the cSH2 domain for interaction with the TIM barrel (autoinhibited) and the phosphorylated X−Y linker (active).

MATERIALS AND METHODS

Cloning and Purification of the cSH2 Domain of PLC-γ1. The cSH2 domain (amino acids 664−766) was amplified from full-length rat PLC-γ1 by polymerase chain reaction and then subcloned into a modified pET15b vector, which incorporates a His_6 tag and a tobacco etch virus (TEV) protease site at the N-terminus of the expressed protein. The cSH2 domain was expressed in the BL21 strain of *Escherichia coli* and purified as described previously with the following modifications.[9] After TEV cleavage, the sample was applied to a 5 mL HisTrap HP column (GE Healthcare). Flow-through fractions were pooled and diluted 5-fold into 20 mM HEPES (pH 7.5), 300 mM NaCl, and 5% (v/v) glycerol. The sample was further diluted 3-fold into buffer S1 [20 mM HEPES (pH 7.5), 1 mM DTT, and 5% (v/v) glycerol] and applied to an 8 mL SourceS cation exchange column equilibrated in 10% buffer S2 [20 mM HEPES (pH 7.5), 1 M NaCl, 1 mM DTT, and 5% (v/v) glycerol]. Bound proteins were eluted with a linear gradient from 10 to 100% buffer S2 over 20 column volumes.

Crystallization of the cSH2 Domain of PLC-γ1. Diffraction quality crystals of the PLC-γ1 cSH2 domain were obtained by hanging drop vapor diffusion at 4 °C. Drops were formed by mixing 2 μL of the cSH2 domain at 7.5 mg/mL in 20 mM HEPES (pH 7.5), 150 mM NaCl, 1 mM DTT, and 5% (v/v) glycerol with 1 μL of the reservoir solution [100 mM MES (pH 5.5), 200 mM ammonium acetate, and 25% (w/v) PEG 4000]. Single crystals appeared within 2 days, grew to maximal size (~200 μm on the longest edge) within 1 week, and had a Matthews coefficient (V_m) of 1.94 Å^3/Da. The space group and unit cell parameters are listed in Table 1. Crystals were cryoprotected by being flash-cooled in liquid nitrogen.

Crystallization of the cSH2 Domain of PLC-γ1 Bound to the pTyr783 Peptide. The PLC-γ1 cSH2 domain−pTyr783 peptide complex was formed by incubating the cSH2 domain (7.5 mg/mL) with a 1.1-fold molar excess of the pTyr783 peptide (1.4 mg/mL) in 20 mM HEPES (pH 7.5), 150 mM NaCl, 1 mM DTT, and 5% (v/v) glycerol at 4 °C for 1 h prior to the initiation of crystallization trials. Crystals were obtained at 20 °C by microseeding hanging drops with crushed crystals of the apo-cSH2 domain. Crystals grew from drops formed by mixing 1 μL of protein solution with 2 μL of the reservoir solution [100 mM MES (pH 6.0), 200 mM ammonium acetate, and 35% (w/v) PEG 4000], reached a maximal length of ~250 μm within 2 weeks, and had a V_m of 1.62 Å^3/Da. The space group and unit cell parameters are listed in Table 1. Crystals were cryoprotected by being flash-cooled in liquid nitrogen.

Data Collection and Structure Determination. Native sets of X-ray diffraction data were collected on single crystals of the apo-cSH2 domain and the cSH2 domain bound to the pTyr783 peptide on SER-CAT beamline 22-ID at the Advanced Photon Source at Argonne National Laboratory (Argonne, IL). Data were collected on a MAR300 CCD detector, at a crystal to detector distance of 150 mm. One scan about ω totaling 200° was collected for each crystal. Each frame consisted of a 0.5° rotation taken for 1 s. Data were indexed, integrated, and scaled using HKL2000.[11] Phases were solved by

Table 1. Data Collection and Refinement Statistics for the PLC-γ1 cSH2 Domain and the PLC-γ1 cSH2 Domain Bound to the pTyr783 Peptide[a]

	PLC-γ1 cSH2	PLC-γ1 cSH2−pTyr783 peptide
Data Collection		
space group	$C222_1$	$P2_12_12_1$
unit cell dimensions		
a, *b*, *c* (Å)	48.1, 53.3, 150.3	29.0, 54.5, 59.9
α, β, γ (deg)	90.0, 90.0, 90.0	90.0, 90.0, 90.0
resolution (Å)	35.7−1.70 (1.73−1.70)	40.3−1.50 (1.53−1.50)
no. of unique reflections	21853 (1066)	15900 (763)
R_{merge}[b]	6.1 (46.3)	6.7 (33.1)
$\langle I/\sigma \rangle$[c]	33.3 (4.7)	29.1 (3.8)
completeness (%)	99.3 (91.1)	99.8 (97.4)
redundancy	8.0 (8.0)	7.3 (4.7)
wavelength (Å)	1.000	0.979
no. of molecules in the asymmetric unit	2	1
Refinement		
resolution (Å)	35.7−1.70	40.3−1.50
no. of reflections (test set/working set)	1120/20696	790/15060
R/R_{free}[d]	18.4/22.3	16.3/19.8
no. of atoms		
protein	1721	851
peptide	−	68
water	103	80
rmsd		
bond lengths (Å)	0.007	0.015
bond angles (deg)	1.09	1.63
average *B* factor (Å^2)		
protein	27.8	14.0
peptide	−	27.4
water	29.0	25.3
Ramachandran plot (%)		
favored	96	97
allowed	4	3
disallowed	0	0
PDB entry	4K44	4K45

[a]Numbers in parentheses refer to data for the highest-resolution shell. Each data set was collected from a single crystal. [b]$R_{merge} = 100\sum|I - \langle I \rangle|/\sum I$, where I is the integrated intensity of a measured reflection. [c]$\langle I/\sigma \rangle$ is the mean signal-to-noise ratio, where I is the integrated intensity of a measured reflection and σ is the estimated error in the measurement. [d]$R = 100\sum|F_o - F_c|/\sum F_o$, where F_o and F_c are the observed and calculated structure factor amplitudes, respectively. R_{free} is calculated as R using 5% of the total reflections that have been randomly excluded from refinement.

dx.doi.org/10.1021/bi400433b | *Biochemistry* 2013, 52, 4810−4819

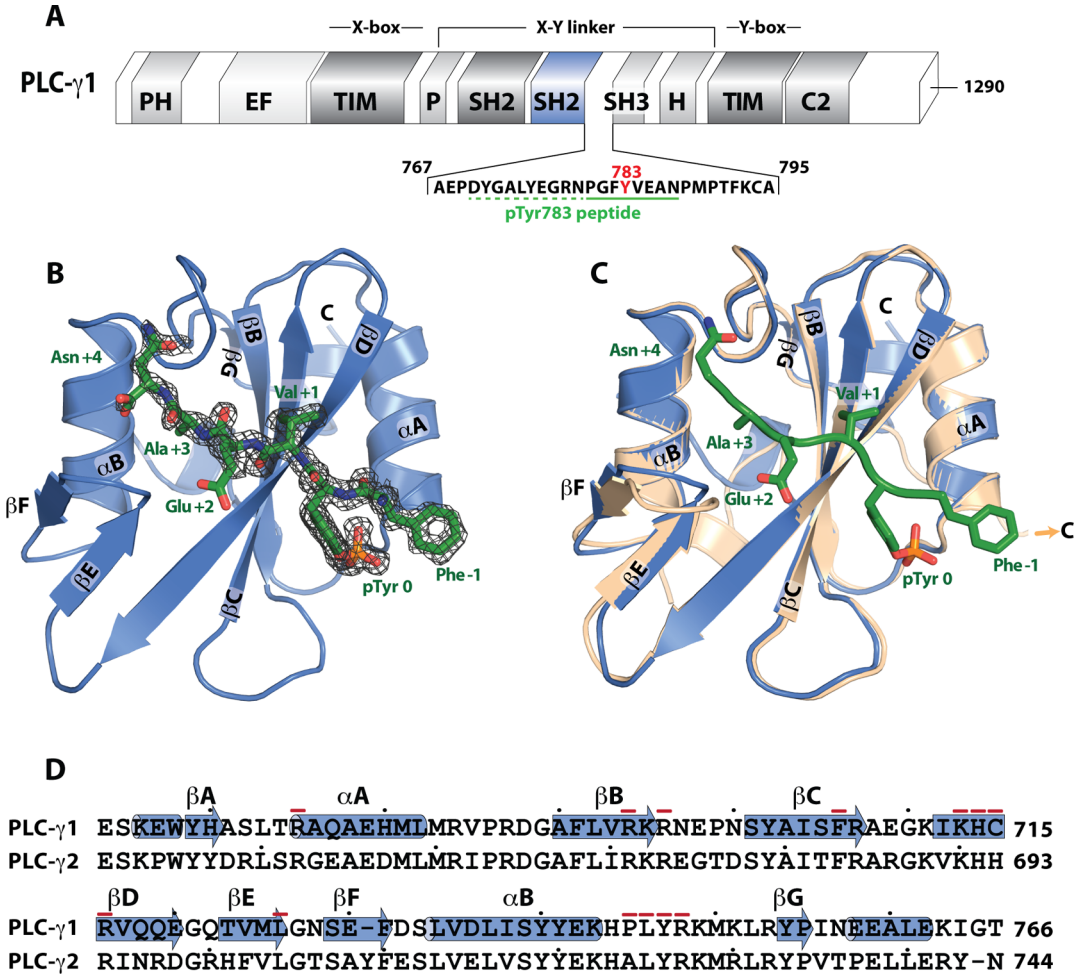

Figure 1. Crystal structures of the C-terminal SH2 domain of PLC-γ1. (A) Schematic representation of full-length rat PLC-γ1. Highlighted are the C-terminal SH2 domain (blue) and the primary sequence of the phosphorylated peptide (green underline, phosphorylated Tyr783 is red) used for structure determination. The dashed green line indicates the portion of the peptide disordered in the crystal structure. (B) Structure of the cSH2 domain of PLC-γ1 bound to the pTyr783 peptide. Elements of secondary structure within the cSH2 domain are labeled according to the established nomenclature. The bound peptide is colored green with associated electron density ($2F_o - F_c$ map contoured at 1.0σ) shown as black mesh. Positions of amino acids within the peptide are numbered relative to the phosphotyrosine. (C) Structural comparison of the cSH2 domain in the presence (blue) and absence (wheat) of the pTyr783 peptide. Structures superimposed (rmsd ~0.3 Å) for 77 equivalent Cα atoms. (D) Alignment of the primary sequences of the cSH2 domain from rat PLC-γ1 and PLC-γ2. α-Helices (cylinders) and β-strands (arrows) are assigned using the structure of the peptide-bound form of the cSH2 domain. Dots denote every 10th residue, and residues that contact the pTyr783 peptide are denoted with a red dash.

molecular replacement using Phaser in the CCP4 program suite.[12,13] The coordinates of the cSH2 domain of PLC-γ1 (PDB entry 3GQI) were used as a search model for the apo-cSH2 domain. After partial refinement of the apo-cSH2 domain structure, these phases were used to identify a solution for the cSH2 domain bound to the pTyr783 peptide. Both models were subjected to multiple rounds of restrained refinement and TLS refinement using Refmac5, as well as manual refinement in Coot.[14,15] A final round of restrained refinement and TLS refinement was conducted in Phenix.[16] The stereochemical quality of each model was assessed with MolProbity.[17] Complete data collection and structure refinement statistics are listed in Table 1.

Cloning of PLC-γ1 Point Mutants. The R675E, K711E/K713E, R716E, N728E, Y747E/R748E, D342K, E347K, D370K, and D1019K point mutations were introduced into rat PLC-γ1 in a modified pcDNA3.1 vector, which incorporates an HA tag at the N-terminus of the expressed protein, by QuikChange site-directed mutagenesis (Stratagene). Incorporation of each mutation was confirmed by automated DNA sequencing of the entire PLC-γ1 open reading frame.

Measurement of PLC-γ1 Activity. Cell-based assays for measuring the accumulation of [^{3}H]inositol phosphates were performed as described previously.[3,5,9] Briefly, HEK293 cells were transfected with plasmids encoding HA-tagged PLC-γ1 constructs using Fugene-6 (Promega). Twenty-four hours post-transfection, cells were metabolically labeled with 1 μCi of [^{3}H] *myo*-inositol in serum-free, inositol-free DMEM for 16 h followed by a 1 h incubation in the presence of 10 mM LiCl. For experiments in which cells were treated with LiCl overnight, 10 mM LiCl was added to the radiolabeling medium. To measure PLC activity in response to EGF stimulation, cells were cotransfected with 200 ng of the indicated PLC-γ1 construct and 100 ng of plasmid encoding the human EGF receptor (a generous gift from Dr. H. Shelton Earp, The University of North Carolina at Chapel Hill). Cells were stimulated with recombinant human EGF (Invitrogen) for 30 min in the presence of 10 mM LiCl. Cells were lysed with

dx.doi.org/10.1021/bi400433b | *Biochemistry* 2013, 52, 4810−4819

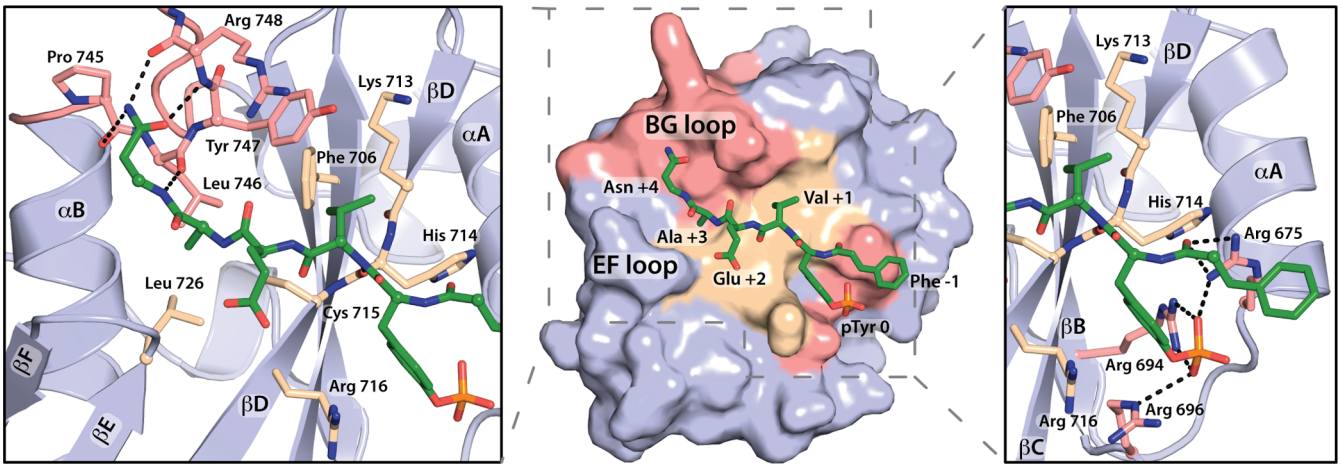

Figure 2. The BG loop forms part of the interface with the pTyr738 peptide. The surface of the cSH2 domain (middle) is colored to highlight the BG loop and phosphotyrosine-binding pocket (pink) as well as intervening residues (wheat) that interact with the peptide. The left and right panels detail interactions between the peptide and the cSH2 domain; dashed lines represent hydrogen bonds.

formic acid, and following neutralization with ammonium hydroxide, the lysate was applied to Dowex columns. Accumulation of [^{3}H]inositol phosphates was measured by liquid scintillation counting. Expression of PLC-γ1 constructs was assessed by Western blotting. Cell lysates were probed with a monoclonal antibody against the HA epitope (clone 3F10, Roche). As a loading control, lysates were also probed with an antibody against β-actin (clone AC-15, Sigma-Aldrich).

Homology Modeling and Electrostatic Surface Calculation. A homology model of PLC-γ1 (amino acids 1−1219) lacking the X−Y linker (amino acids 471−983) was generated using the Phyre server.[18] Electrostatic surfaces were calculated using APBS executed within PyMOL.[19,20]

Protein and Peptide Concentrations. Concentrations of the cSH2 domain were determined using A_{280} and the extinction coefficient calculated using ProtParam (ε = 14400 M^{-1} cm^{-1}). Concentrations of the pTyr783 peptide were calculated using A_{267} and an extinction coefficient ε of 2752 M^{-1} cm^{-1} calculated by adding the extinction coefficients of tyrosine (ε = 1050 M^{-1} cm^{-1}) and phosphotyrosine (ε = 652 M^{-1} cm^{-1}). The pTyr783 peptide (acetyl-DYGALYEGRNPG-F<u>Y</u>VEAN-amide, phosphorylated tyrosine underlined) was synthesized by Creative Peptides Inc. (Shirley, NY).

RESULTS

Phosphorylation of PLC-γ1 at Tyr783 increases lipase activity, and we previously suggested that this increase results from intramolecular interaction of the cSH2 domain with the phosphorylated form of Tyr783 found immediately C-terminal to the cSH2 domain. To improve our understanding of this regulation, we determined the crystal structure of the cSH2 domain of PLC-γ1 in isolation as well as in complex with a peptide encompassing the region surrounding pTyr783 (Figure 1).

The structure of the apo form of the cSH2 domain was determined by molecular replacement, using the structure of the cSH2 domain of PLC-γ1 (PDB entry 3QGI) as a search model, and refined at a resolution of 1.7 Å (Table 1). Phases from this model were subsequently used to refine the 1.5 Å resolution structure of the peptide-bound form (Table 1).

The structure of the cSH2 domain is similar to those of other SH2 domains and consists of a central antiparallel β-sheet flanked by two α-helices (Figure 1B). The phosphopeptide binds in an extended groove roughly orthogonal to the central β-sheet and is anchored at one end by the phosphorylated tyrosine in a deep pocket on the cSH2 domain. Although the phosphopeptide consists of 18 residues, only the C-terminal eight have clear electron density in the structure and bury ∼430 Å^2 of the solvent-accessible surface of the cSH2 domain upon complex formation. The remainder of the peptide is presumably disordered and not required for complex formation. The extended interface is recapitulated in other peptide−SH2 domain complexes.[21,22]

Conformational differences between the peptide-bound and unbound forms of the cSH2 domain (Figure 1C) are unlikely to be functionally important. For instance, the largest differences between the two forms occur at the termini of the cSH2 domain on the opposite side of the domain relative to the bound peptide. The N-terminal helix reorients, and the C-terminal helix is missing in the unbound form. However, these conformational changes do not propagate to the site of the bound peptide, suggesting that the termini are inherently flexible. Additionally, the EF loop is translated ∼2.5 Å toward the bound peptide relative to the unbound form, but this difference is ascribed to interactions of this loop with the C-terminus of a symmetry mate in the crystal of the unbound form.

The two structures superimpose with an rmsd of ∼0.3 Å for 77 equivalent Cα atoms. In particular, the conformations of the BG loop and βG strand are essentially identical between the two structures. We previously postulated that conformational changes centered within this region in response to engagement of the phosphopeptide would be linked to the release of autoinhibition of phospholipase activity.[9]

While the conformations of the BG loop and βG strand remain unaltered between the two structures, the BG loop substantially contributes to the interface with the phosphopeptide (Figure 1D). For example, Asn +4 of the phosphopeptide, corresponding to residue 787 in full-length PLC-γ1, participates in four hydrogen bonds with the BG loop (Figure 2). Leu746 within the BG loop also forms part of the hydrophobic groove that interacts with Ala +3 of the phosphopeptide. The remainder of the hydrophobic groove of the cSH2 domain is occupied by Val +1 of the phosphopeptide before terminating in the phosphotyrosine-binding pocket where pTyr783

dx.doi.org/10.1021/bi400433b | *Biochemistry* 2013, 52, 4810−4819

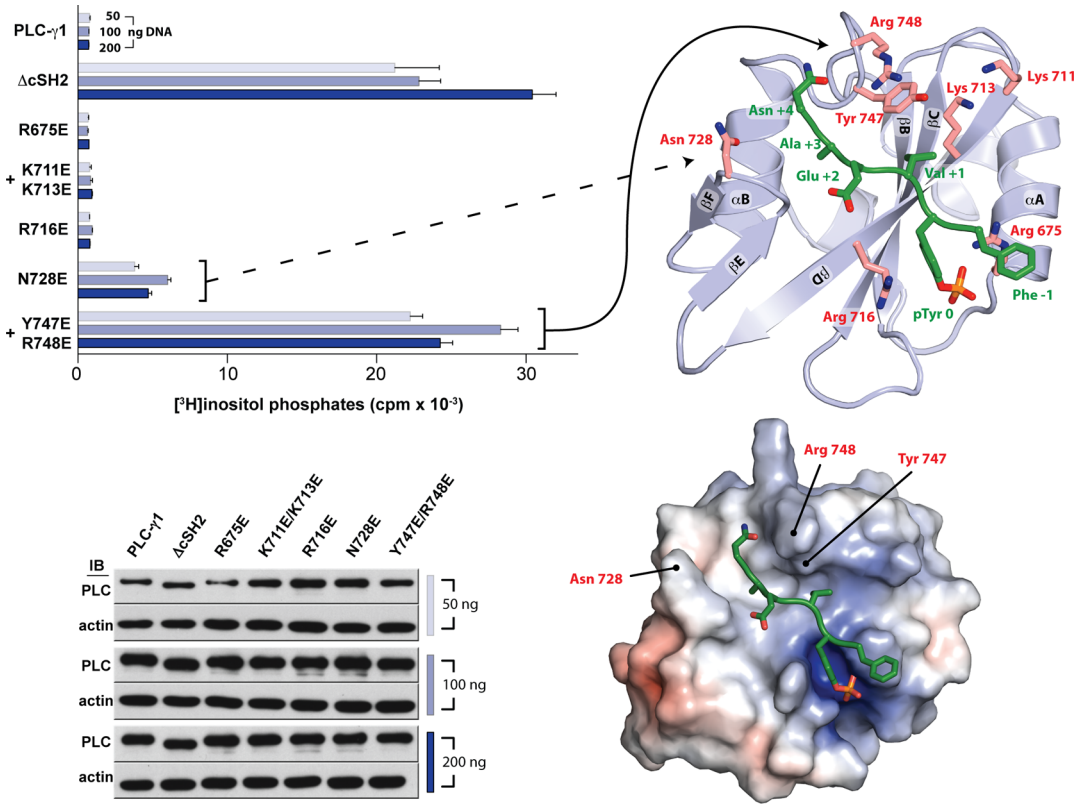

Figure 3. Autoinhibitory interface within the cSH2 domain maps to the electropositive EF and BG loops. HEK293 cells were transfected with the indicated amounts of plasmids encoding either wild-type or mutant forms of PLC-γ1 prior to quantification of accumulated [^{3}H]inositol phosphates (top left). Mutated residues are highlighted on the structure of the cSH2 domain (top right). Data are presented as means ± SEM of triplicate samples from a single experiment and are representative of three independent experiments. Expression of PLC-γ1 constructs confirmed by Western blots of cell lysates (bottom left). Mutated residues that increase basal phospholipase activity are indicated on the solvent-accessible surface of the cSH2 domain (bottom right), colored according to electrostatic potential calculated without the bound peptide (red, $-5kT/e$; blue, $5kT/e$).

interacts with four arginines (Arg675, Arg694, Arg696, and Arg716).

The structures of the bound and unbound forms of the cSH2 domain fail to highlight conformational changes that can be reasonably linked to the enhancement of phospholipase activity. However, a likely alternative posits that the peptide-binding surface of the cSH2 domain directly occludes the active site of PLC-γ1. In this case, engagement of the cSH2 domain by a phosphopeptide would directly disrupt this occlusion to release autoinhibition. This idea was tested by mutating the peptide-binding surface of the cSH2 domain within the context of full-length PLC-γ1 and measuring phospholipase activity in cells after metabolic labeling of phosphoinositide pools (Figure 3). Several substitutions of positively charged residues with glutamic acid had no effect on basal phospholipase activity. This set includes the individual substitution of two arginines (Arg675 and Arg716) within the pocket that binds pTyr783 as well as double substitution of lysines (Lys711 and Lys713) adjacent to this pocket. In contrast, mutation of the EF loop (N728E) enhanced basal phospholipase activity approximately 5-fold, and a tandem substitution (Y747E/R748E) within the BG loop activated PLC-γ1 by >30-fold. This elevated basal activity approximates the activity of PLC-γ1 lacking the entire cSH2 domain [ΔcSH2 (Figure 3)], which we have shown completely lacks autoinhibition mediated by the X−Y linker.[9] These results further emphasize the importance of the BG loop and adjacent regions of the cSH2 domain in the autoinhibition of PLC-γ isozymes and suggest that these regions may interact with the active site to autoinhibit phospholipase activity. Conversely, the pocket required to bind pTyr783 likely does not interact with the active site to autoinhibit PLC-γ1. However, this pocket is nevertheless essential for activation because the cSH2 domain must engage pTyr783 and the surrounding peptide to relieve autoinhibition as shown previously.[9]

The surface of the cSH2 domain, including the BG loop, that engages the pTyr783 peptide is positively charged (Figure 3). If this surface directly occludes the active site of PLC-γ1 to autoinhibit phospholipase activity, it seems reasonable to expect the complementary surface of PLC-γ1 to be negatively charged. In an effort to identify potential areas near the active site of PLC-γ1 that interact with the cSH2 domain, a homology model of PLC-γ1 was generated based on the structure of PLC-β3 (Figure 4). This model spans the PH to C2 domains but lacks the X−Y linker. Comparison of this model with the structure of PLC-β3 highlights several negative patches in the vicinity of the active site of PLC-γ1 that are not found in PLC-β3. Negatively charged residues within these areas of PLC-γ1 were mutated to lysine, and the phospholipase activity of the resulting mutants was quantified in cells.

Individual substitutions at two positions (D342K and E347K) produced modest enhancement (2−5-fold) of basal phospholipase activity relative to that of the wild-type isozyme (Figure 4). More interestingly, substitution of Asp1019 with lysine enhanced basal phospholipase activity approximately 15-fold. In comparison, the phospholipase activity of PLC-

dx.doi.org/10.1021/bi400433b | Biochemistry 2013, 52, 4810−4819

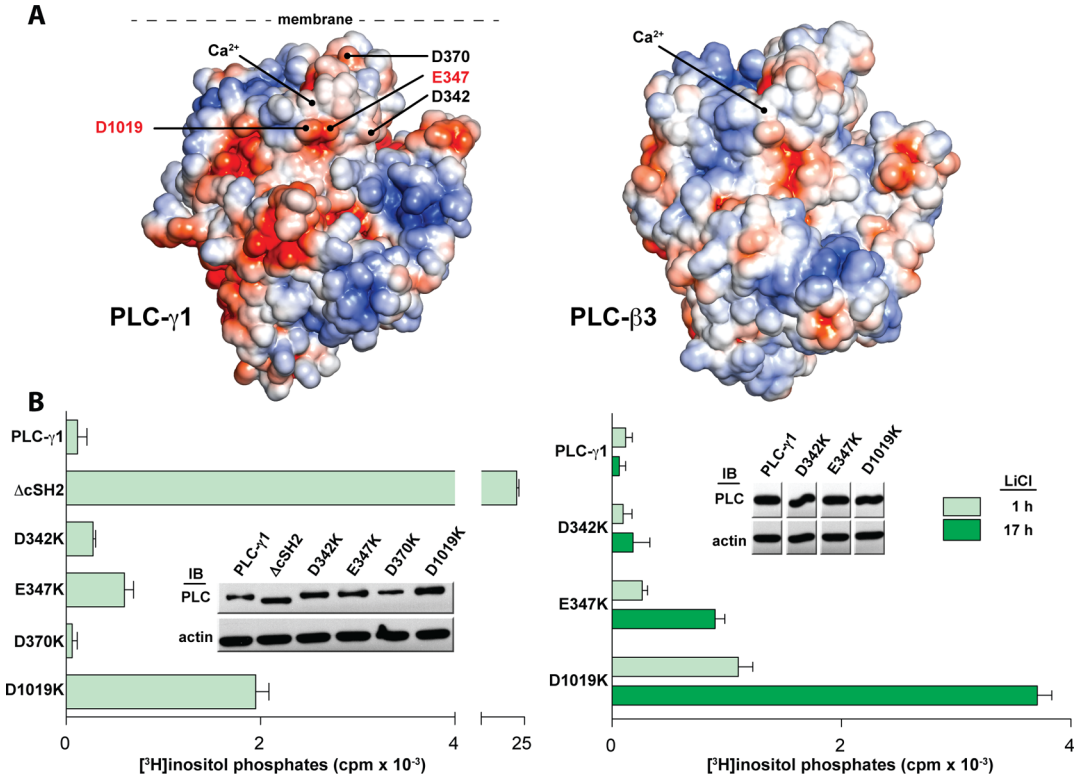

Figure 4. The catalytic core of PLC-γ1 contains a putative interface with the cSH2 domain. (A) The core of PLC-γ1 is electronegative. The solvent-accessible surface of a homology model of PLC-γ1 lacking the X−Y linker (left) is colored according to electrostatic potential (red, $-5kT/e$; blue, $5kT/e$). Residues selected for mutational analysis are labeled. The equivalent representation of PLC-β3 is shown at the right. (B) Mutations near the active site of PLC-γ1 increase basal activity. HEK293 cells were transfected with plasmids encoding either wild-type PLC-γ1 or PLC-γ1 harboring the indicated mutations in the TIM barrel. Accumulation of [^{3}H]inositol phosphates was quantified after a 1 h incubation with LiCl (left) or for the indicated times (right). The amount of radioactivity that accumulated in cells transfected with the empty vector was subtracted from all measurements. Data are presented as means ± SEM of triplicate samples from a single experiment. Expression of PLC-γ1 constructs was verified by Western blots (insets).

γ1(ΔcSH2), which completely lacks autoinhibition mediated by the X−Y linker, is increased by approximately 130-fold. To assess further these relatively small increases in phospholipase activity, a second set of cells were treated identically except with a prolonged incubation (17 h) with LiCl to enhance accumulation of inositol phosphates. Under these conditions, the phospholipase activity of PLC-γ1(E347K) was increased by approximately 15-fold relative to that of wild-type PLC-γ1; the activity of PLC-γ1(D1019K) was approximately 60-fold higher. These results are consistent with the proposal that Glu347 and Asp1019 interact with the cSH2 domain to autoinhibit PLC-γ1. These two sites are separated by the X−Y linker in the primary sequence of PLC-γ1 but are adjacent to each other in the homology model.

The relative basal phospholipase activities of PLC-γ1-(Y747E/R748E) and PLC-γ1(D1019K) measured in intact cells were confirmed with purified proteins. These proteins, along with wild-type PLC-γ1, were purified to homogeneity after expression in insect cells and their specific activities compared using 30 μM [^{3}H]PtdIns(4,5)P_2. Consistent with the intact cell experiments, wild-type PLC-γ1 had a low basal activity (0.72 ± 0.25 pmol min^{-1} ng^{-1}); PLC-γ1(D1019K) possessed a slightly elevated phospholipase activity (3.98 ± 0.23 pmol min^{-1} ng^{-1}), and PLC-γ1(Y747E/R748E) was highly active (42.5 ± 10.85 pmol min^{-1} ng^{-1}) (data not shown).

These mutational analyses suggest that the cSH2 domain directly interacts with the active site of PLC-γ1 to autoinhibit phospholipase activity. However, it was also important to assess the effects of these mutations on phosphorylation-induced activation. Thus, we examined the capacity of the epidermal growth factor receptor (EGFR) to activate a panel of the PLC-γ1 mutants in HEK293 cells (Figure 5).

Concentration-dependent activation of phospholipase C by epidermal growth factor (EGF) was observed in HEK293 cells cotransfected with wild-type PLC-γ1 and EGFR (Figure 5A). Maximal activation was observed with approximately 50 nM EGF. In contrast, transient expression of either PLC-γ1 or EGFR alone resulted in minimal responses to EGF. As expected, PLC-γ1(ΔcSH2) was not further activated by 50 nM EGF when co-expressed with the EGFR (Figure 5B). Of the panel of PLC-γ1 mutants harboring substitutions (Figure 5B), only two (R675E and R716E) could not be activated to the same extent as wild-type PLC-γ1 by application of 50 nM EGF after cotransfection with EGFR. Both of these sites reside in the pocket of the cSH2 domain needed to engage phosphotyrosine and likely prevent activation by reducing the capacity of the cSH2 domain to bind pTyr783. Under identical conditions, the remaining substituted forms retained the capacity to be activated fully by addition of EGF. Indeed, these mutants, which include substitutions within both the cSH2 domain and TIM barrel, consistently exhibited phospholipase activity in response to EGF that surpassed the

dx.doi.org/10.1021/bi400433b | Biochemistry 2013, 52, 4810−4819

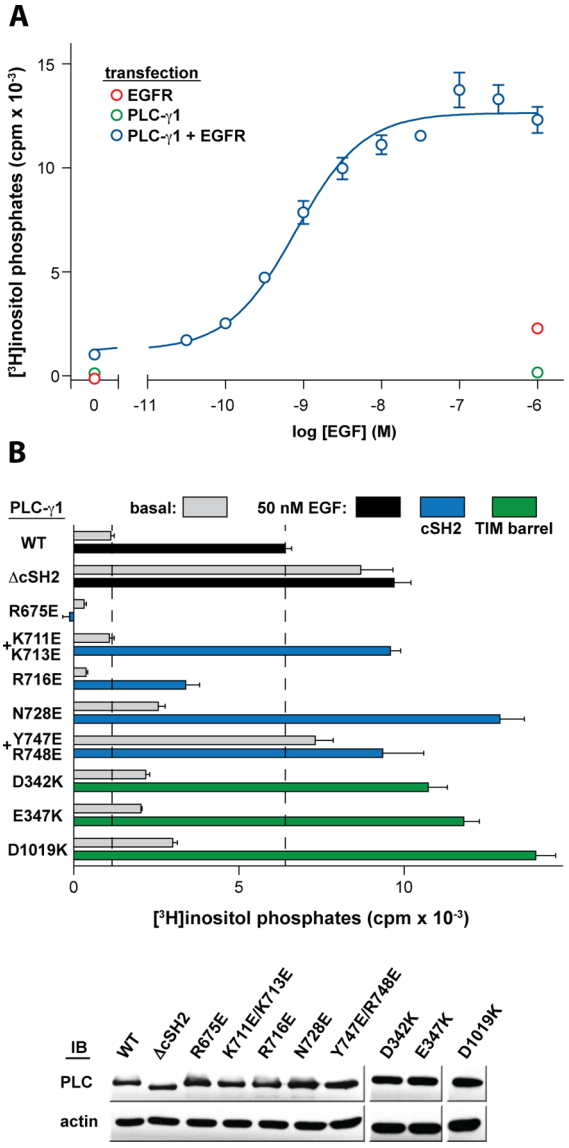

Figure 5. PLC-γ1 is activated to a similar extent by either EGFR-dependent phosphorylation or mutation of the BG loop. (A) Dose-dependent accumulation of inositol phosphates by EGF in cells overexpressing EGFR and PLC-γ1. HEK293 cells were transfected with plasmids encoding PLC-γ1, EGFR, or both constructs as indicated prior to challenge with EGF for 30 min and measurement of [^{3}H]inositol phosphates. In each case, the level of radioactivity that accrued in cells not treated with LiCl was subtracted from all values. (B) Stimulation of PLC-γ1 by EGF is not further enhanced by mutation of the BG loop. HEK293 cells were cotransfected with plasmids encoding EGFR and either wild-type PLC-γ1 or the indicated mutant forms. Accumulation of [^{3}H]inositol phosphates was quantified after a 30 min challenge with vehicle (gray bars) or 50 nM EGF (black, blue, and green bars). The amount of radioactivity that accumulated in cells overexpressing EGFR following treatment with either vehicle or EGF was subtracted from each basal or EGF-treated condition, respectively. Activities of PLC-γ1 forms harboring mutations in either the cSH2 domain or the TIM barrel were measured independently and the results combined into a single graph for the sake of clarity. Expression of PLC-γ1 constructs verified by Western blots of cell lysates (bottom). Data are presented as means ± SEM of triplicate samples from single experiments and are representative of three independent experiments in panel B.

equivalent activity of wild-type PLC-γ1 and approached or exceeded the phospholipase activity of PLC-γ1(ΔcSH2). These data indicate a residual autoinhibition of phosphorylated, wild-type PLC-γ1 that can be relieved by either deletion of the cSH2 domain or mutations that prevent its interaction with the active site.

DISCUSSION

The structure of the cSH2 domain is not substantially altered upon engagement of the pTyr783 peptide, and in particular, the BG loop and βG strand adopt an essentially identical configuration in the presence and absence of the phosphopeptide (Figure 1C). However, the BG loop makes a substantial contribution to the interface with the pTyr783 peptide (Figure 2). Therefore, these data strongly suggest that phosphorylated sequences and the lipase active site directly compete for binding to overlapping surfaces of the cSH2 domain, and that in contrast to our previous supposition,[9] no conformational changes within the cSH2 domain are required to regulate phospholipase activity.

The model driven by the structures of the cSH2 domain with and without bound pTyr783 peptide shares many features with the autoinhibition of class I PI 3-kinases.[23−25] Indeed, the enzymatic activity of the catalytic p110 subunit is autoinhibited by tandem SH2 domains in the regulatory subunit, p85. Structures of p85−p110 complexes indicate that the nSH2 domain engages the helical and kinase domains of p110 through the same surface that binds phosphopeptides.[26,27] Biochemical studies suggest that positively charged residues that form the phosphopeptide-binding site on the nSH2 domain engage a cluster of acidic residues within the helical domain of p110 to autoinhibit kinase activity.[28] These positively charged residues in the nSH2 domain also directly contact bound phosphopeptides, suggesting that binding of the nSH2 domain to p110 and phosphorylated target sequences is mutually exclusive.[29] Charge reversal mutations within the interface between the nSH2 domain and p110 are sufficient to increase kinase activity *in vitro*.[28] Although the binding mode between the nSH2 domain and p110 is well-defined, the precise mechanism by which disruption of this autoinhibitory interface is translated into enhanced enzymatic activity remains to be fully elucidated. Nevertheless, phosphorylated peptides derived from receptor tyrosine kinases and adaptor proteins activate PI 3-kinase *in vitro*, and oncogenic missense mutations in p110 were mapped to the autoinhibitory interface with the nSH2 domain.[30−35]

We have identified a positively charged surface of the cSH2 domain that is critically involved in autoinhibition of PLC-γ1 activity (Figure 3). The corresponding portion of the PLC-γ2 cSH2 domain is also highly electropositive, suggesting a conserved mode of regulation (data not shown). Mutational analysis of the TIM barrel suggests the presence of a complementary, i.e., negatively charged, surface that is involved in the regulation of lipase activity (Figure 4). The nSH2 domain of p85 autoinhibits p110 activity *in trans*. In contrast, PLC-γ1 activity is autoinhibited by an intramolecular interaction that requires the cSH2 domain. Nevertheless, we posit that the cSH2 domain of PLC-γ1 and the nSH2 domain of p85 autoinhibit enzymatic activity through a similar mechanism. In the basal state, the surface of the cSH2 domain that binds phosphorylated sequences, specifically the BG and EF loops, directly engages the TIM barrel such that access of the substrate to the lipase active site is precluded. Upon nSH2

dx.doi.org/10.1021/bi400433b | *Biochemistry* 2013, 52, 4810−4819

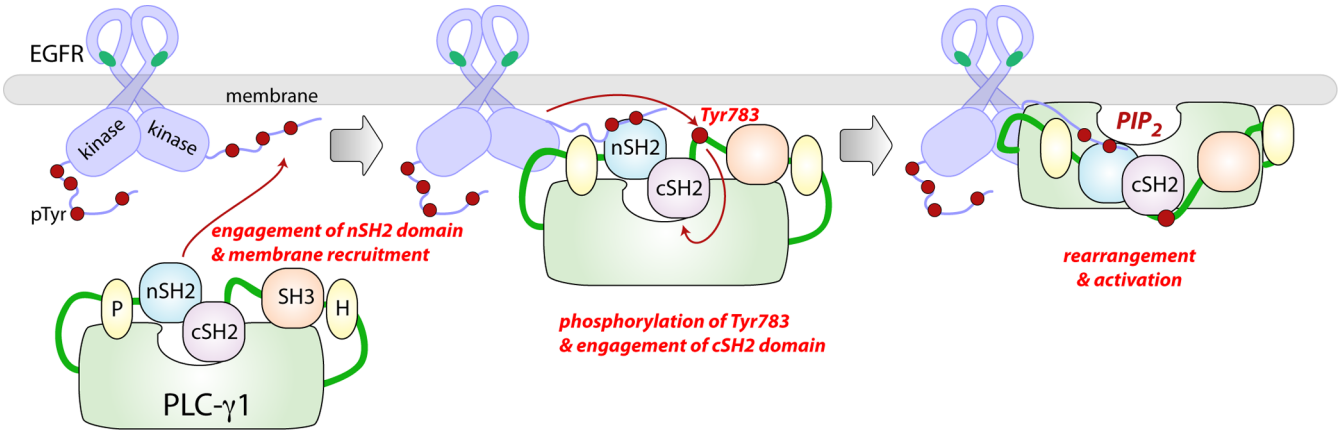

Figure 6. Model for the phosphorylation-dependent activation of PLC-γ1. In the basal state, the catalytic TIM barrel (light green) of PLC-γ1 is autoinhibited by the cSH2 domain within the X−Y linker. The phosphorylated tails of activated RTKs (red circles), such as EGFR, provide docking sites for the nSH2 domain, resulting in the recruitment of PLC-γ1 to the plasma membrane. PLC-γ1 is subsequently phosphorylated on Tyr783 within the X−Y linker, which results in an intramolecular association with the cSH2 domain. This interaction leads to conformational changes within the larger X−Y linker that are coupled to the release of autoinhibition and enhanced hydrolysis of the substrate PtdIns(4,5)P_2 (PIP_2).

domain-dependent recruitment to activated RTKs, PLC-γ1 is phosphorylated on specific tyrosines, e.g., Tyr783. Phosphorylated Tyr783 then engages the cSH2 domain, disrupting the interaction with the TIM barrel and allowing enhanced phospholipase activity (Figure 6).

In-frame deletions in the cSH2 domain of PLC-γ2 were linked recently to immune system dysregulation in a cohort of patients with a dominantly inherited syndrome characterized by immunodeficiency and autoimmunity.[36] Cell-based overexpression studies as well as *ex vivo* analysis of primary immune cells from patients indicated that these deleted forms of PLC-γ2 are hyperactive. Genetic analysis of affected individuals identified two distinct deletion variants of PLC-γ2. One variant lacks a portion of the cSH2 domain encompassing the EF and BG loops. These loops play a central role in mediating the autoinhibition of PLC-γ1 activity. Therefore, the absence of these elements provides a clear rationale for the observed increases in PLC-γ2 activity. The other deleted form of PLC-γ2 lacks approximately 40 amino acids at the N-terminus of the cSH2 domain. In this case, elevated lipase activity is likely attributable to unfolding of the cSH2 domain and the concomitant loss of the surface required for autoinhibition.

The autoinhibitory interface within the cSH2 domain is apparently centered on the BG loop. However, a single point mutation in the EF loop, N728E, increased basal PLC-γ1 activity approximately 5-fold (Figure 3), suggesting that this loop also makes a contribution to the autoinhibitory surface. Alanine-scanning mutagenesis of individual amino acids, including Asn728, across the EF loop did not result in mutants of PLC-γ1 with altered basal phospholipase activity.[9] Apparently, the neutral N728A mutation is insufficient to disrupt the autoinhibitory interface between the cSH2 domain and catalytic core.

Genetic evidence supports the notion that the surface of the cSH2 domain encompassing the EF loop is involved in the autoinhibition of PLC-γ isozymes. A single missense mutation, S707Y, located in strand βE of the PLC-γ2 cSH2 domain was linked to a distinct group of patients with dominantly inherited autoinflammatory disease.[37] The equivalent residue in PLC-γ1, Ser729, is immediately adjacent to Asn728. Concordant with our observation that the N728E mutation increases the basal activity of PLC-γ1, several lines of evidence suggest that S707Y is a gain-of-function substitution in PLC-γ2. Zhou and colleagues suggest that the altered activity of PLC-γ2(S707Y) is due to insertion of a putative phosphorylation site within the cSH2 domain. However, we posit that point mutations in the EF loop (N728E in PLC-γ1) and βE strand (S707Y in PLC-γ2) increase the activity of PLC-γ isozymes through a common mechanism, disruption of the autoinhibitory interface between the cSH2 domain and the catalytic core.

Forward genetic screens in mice also implicate residues outside of the cSH2 domain in the regulation of PLC-γ2 activity. One such screen identified a missense mutation, D993G, in the TIM barrel of PLC-γ2 that is linked to spontaneous inflammation, autoimmunity, and arthritis.[38] B cells derived from mice heterozygous for this mutation are hyper-responsive to receptor activation *ex vivo*, suggesting that D993G is a gain-of-function mutation. Indeed, subsequent analysis of PLC-γ2(D993G) in an overexpression system demonstrated that this mutant isozyme exhibits higher basal and receptor-dependent activity than wild-type PLC-γ2 in cells.[39] Consistent with these findings, we observed that PLC-γ1 harboring a mutation at Asp1019, which corresponds to Asp993 in PLC-γ2, had elevated basal activity (Figure 4). The D1019K mutation also potentiated the EGFR-dependent activation of PLC-γ1 in cells (Figure 5). Given that these effects resulted from a charge reversal mutation, it is tempting to speculate that Asp1019 interfaces with the positively charged surface of the cSH2 domain to autoinhibit PLC-γ1 activity.

The cSH2 domain is the primary determinant mediating autoinhibition of PLC-γ1, and we have focused on how this domain responds to the engagement of phosphorylated Tyr783 to regulate phospholipase activity. However, the cSH2 domain operates within the context of the larger X−Y linker, and structure determination of a full-length form of PLC-γ1 will be required to fully understand how tyrosine phosphorylation is coupled to the release of cSH2 domain-mediated autoinhibition in holo-PLC-γ1.

AUTHOR INFORMATION

Corresponding Author

*Department of Pharmacology, UNC School of Medicine, 120 Mason Farm Rd., 4009 Genetic Medicine, CB# 7365, Chapel

Hill, NC 27599-7365. E-mail: sondek@med.unc.edu. Telephone: (919) 966-7530. Fax: (919) 966-5640.

Present Address

[‖]J.R.R.: Boehringer Ingelheim Vetmedica, 2621 North Belt Highway, St. Joseph, MO 64506.

Funding

This work was supported by National Institutes of Health Grants GM057391 (to J.S. and T.K.H.) and GM098894 (to J.S.).

Notes

The authors declare no competing financial interest.

■ ACKNOWLEDGMENTS

We thank Dr. Mischa Machius and Dr. Michael Miley for assistance with the collection of X-ray diffraction data and Dr. H. Shelton Earp for the gift of the EGFR plasmid. We are also indebted to Matthew Barrett for assistance with phospholipase assays and members of the Sondek and Harden laboratories for many helpful suggestions and discussions. Use of the Advanced Photon Source was supported by the U.S. Department of Energy, Office of Science, Office of Basic Energy Sciences, under Contract W-31-109-Eng-38.

■ ABBREVIATIONS

cSH2 domain, C-terminal SH2 domain; EGF, epidermal growth factor; EGFR, epidermal growth factor receptor; Ins(1,4,5)P_3, inositol 1,4,5-trisphosphate; nSH2 domain, N-terminal SH2 domain; PDB, Protein Data Bank; PtdIns(4,5)P_2, phosphatidylinositol 4,5-bisphosphate; PLC, phospholipase C; PH, pleckstrin homology; rmsd, root-mean-square deviation; RTK, receptor tyrosine kinase; SEM, standard error of the mean; SH, Src homology; TIM, triosephosphate isomerase.

■ REFERENCES

(1) Harden, T. K., and Sondek, J. (2006) Regulation of phospholipase C isozymes by Ras superfamily GTPases. *Annu. Rev. Pharmacol. Toxicol. 46*, 355−379.

(2) Rhee, S. G. (2001) Regulation of phosphoinositide-specific phospholipase C. *Annu. Rev. Biochem. 70*, 281−312.

(3) Hicks, S. N., Jezyk, M. R., Gershburg, S., Seifert, J. P., Harden, T. K., and Sondek, J. (2008) General and versatile autoinhibition of PLC isozymes. *Mol. Cell 31*, 383−394.

(4) Jezyk, M. R., Snyder, J. T., Gershberg, S., Worthylake, D. K., Harden, T. K., and Sondek, J. (2006) Crystal structure of Rac1 bound to its effector phospholipase C-β2. *Nat. Struct. Mol. Biol. 13*, 1135−1140.

(5) Waldo, G. L., Ricks, T. K., Hicks, S. N., Cheever, M. L., Kawano, T., Tsuboi, K., Wang, X., Montell, C., Kozasa, T., Sondek, J., and Harden, T. K. (2010) Kinetic scaffolding mediated by a phospholipase C-β and G_q signaling complex. *Science 330*, 974−980.

(6) Nishibe, S., Wahl, M. I., Hernandez-Sotomayor, S. M., Tonks, N. K., Rhee, S. G., and Carpenter, G. (1990) Increase of the catalytic activity of phospholipase C-γ1 by tyrosine phosphorylation. *Science 250*, 1253−1256.

(7) Kim, H. K., Kim, J. W., Zilberstein, A., Margolis, B., Kim, J. G., Schlessinger, J., and Rhee, S. G. (1991) PDGF stimulation of inositol phospholipid hydrolysis requires PLC-γ1 phosphorylation on tyrosine residues 783 and 1254. *Cell 65*, 435−441.

(8) Ozdener, F., Dangelmaier, C., Ashby, B., Kunapuli, S. P., and Daniel, J. L. (2002) Activation of phospholipase Cγ2 by tyrosine phosphorylation. *Mol. Pharmacol. 62*, 672−679.

(9) Gresset, A., Hicks, S. N., Harden, T. K., and Sondek, J. (2010) Mechanism of phosphorylation-induced activation of phospholipase C-γ isozymes. *J. Biol. Chem. 285*, 35836−35847.

(10) Serrano, C. J., Graham, L., DeBell, K., Rawat, R., Veri, M. C., Bonvini, E., Rellahan, B. L., and Reischl, I. G. (2005) A new tyrosine phosphorylation site in PLCγ1: The role of tyrosine 775 in immune receptor signaling. *J. Immunol. 174*, 6233−6237.

(11) Otwinowski, Z., and Minor, W. (1997) Processing of X-ray diffraction data collected in oscillation mode. *Methods Enzymol. 276*, 307−326.

(12) McCoy, A. J., Grosse-Kunstleve, R. W., Adams, P. D., Winn, M. D., Storoni, L. C., and Read, R. J. (2007) Phaser crystallographic software. *J. Appl. Crystallogr. 40*, 658−674.

(13) Winn, M. D., Ballard, C. C., Cowtan, K. D., Dodson, E. J., Emsley, P., Evans, P. R., Keegan, R. M., Krissinel, E. B., Leslie, A. G., McCoy, A., McNicholas, S. J., Murshudov, G. N., Pannu, N. S., Potterton, E. A., Powell, H. R., Read, R. J., Vagin, A., and Wilson, K. S. (2011) Overview of the CCP4 suite and current developments. *Acta Crystallogr. D67*, 235−242.

(14) Murshudov, G. N., Skubak, P., Lebedev, A. A., Pannu, N. S., Steiner, R. A., Nicholls, R. A., Winn, M. D., Long, F., and Vagin, A. A. (2011) REFMAC5 for the refinement of macromolecular crystal structures. *Acta Crystallogr. D67*, 355−367.

(15) Emsley, P., and Cowtan, K. (2004) Coot: Model-building tools for molecular graphics. *Acta Crystallogr. D60*, 2126−2132.

(16) Adams, P. D., Afonine, P. V., Bunkoczi, G., Chen, V. B., Davis, I. W., Echols, N., Headd, J. J., Hung, L. W., Kapral, G. J., Grosse-Kunstleve, R. W., McCoy, A. J., Moriarty, N. W., Oeffner, R., Read, R. J., Richardson, D. C., Richardson, J. S., Terwilliger, T. C., and Zwart, P. H. (2010) PHENIX: A comprehensive Python-based system for macromolecular structure solution. *Acta Crystallogr. D66*, 213−221.

(17) Chen, V. B., Arendall, W. B., III, Headd, J. J., Keedy, D. A., Immormino, R. M., Kapral, G. J., Murray, L. W., Richardson, J. S., and Richardson, D. C. (2010) MolProbity: All-atom structure validation for macromolecular crystallography. *Acta Crystallogr. D66*, 12−21.

(18) Kelley, L. A., and Sternberg, M. J. (2009) Protein structure prediction on the Web: A case study using the Phyre server. *Nat. Protoc. 4*, 363−371.

(19) Baker, N. A., Sept, D., Joseph, S., Holst, M. J., and McCammon, J. A. (2001) Electrostatics of nanosystems: Application to microtubules and the ribosome. *Proc. Natl. Acad. Sci. U.S.A. 98*, 10037−10041.

(20) *The PyMOL Molecular Graphics System*, Version 1.5.0.4, Schrödinger, LLC.

(21) Lee, C. H., Kominos, D., Jacques, S., Margolis, B., Schlessinger, J., Shoelson, S. E., and Kuriyan, J. (1994) Crystal structures of peptide complexes of the amino-terminal SH2 domain of the Syp tyrosine phosphatase. *Structure 2*, 423−438.

(22) Pascal, S. M., Singer, A. U., Gish, G., Yamazaki, T., Shoelson, S. E., Pawson, T., Kay, L. E., and Forman-Kay, J. D. (1994) Nuclear magnetic resonance structure of an SH2 domain of phospholipase C-γ1 complexed with a high affinity binding peptide. *Cell 77*, 461−472.

(23) Yu, J., Zhang, Y., McIlroy, J., Rordorf-Nikolic, T., Orr, G. A., and Backer, J. M. (1998) Regulation of the p85/p110 phosphatidylinositol 3′-kinase: Stabilization and inhibition of the p110α catalytic subunit by the p85 regulatory subunit. *Mol. Cell. Biol. 18*, 1379−1387.

(24) Yu, J., Wjasow, C., and Backer, J. M. (1998) Regulation of the p85/p110α phosphatidylinositol 3′-kinase. Distinct roles for the N-terminal and C-terminal SH2 domains. *J. Biol. Chem. 273*, 30199−30203.

(25) Vadas, O., Burke, J. E., Zhang, X., Berndt, A., and Williams, R. L. (2011) Structural basis for activation and inhibition of class I phosphoinositide 3-kinases. *Sci. Signaling 4*, re2.

(26) Huang, C. H., Mandelker, D., Schmidt-Kittler, O., Samuels, Y., Velculescu, V. E., Kinzler, K. W., Vogelstein, B., Gabelli, S. B., and Amzel, L. M. (2007) The structure of a human p110α/p85α complex elucidates the effects of oncogenic PI3Kα mutations. *Science 318*, 1744−1748.

(27) Mandelker, D., Gabelli, S. B., Schmidt-Kittler, O., Zhu, J., Cheong, I., Huang, C. H., Kinzler, K. W., Vogelstein, B., and Amzel, L. M. (2009) A frequent kinase domain mutation that changes the

interaction between PI3Kα and the membrane. *Proc. Natl. Acad. Sci. U.S.A. 106*, 16996−17001.
(28) Miled, N., Yan, Y., Hon, W. C., Perisic, O., Zvelebil, M., Inbar, Y., Schneidman-Duhovny, D., Wolfson, H. J., Backer, J. M., and Williams, R. L. (2007) Mechanism of two classes of cancer mutations in the phosphoinositide 3-kinase catalytic subunit. *Science 317*, 239−242.
(29) Nolte, R. T., Eck, M. J., Schlessinger, J., Shoelson, S. E., and Harrison, S. C. (1996) Crystal structure of the PI 3-kinase p85 amino-terminal SH2 domain and its phosphopeptide complexes. *Nat. Struct. Biol. 3*, 364−374.
(30) Backer, J. M., Myers, M. G., Jr., Shoelson, S. E., Chin, D. J., Sun, X. J., Miralpeix, M., Hu, P., Margolis, B., Skolnik, E. Y., and Schlessinger, J. (1992) Phosphatidylinositol 3′-kinase is activated by association with IRS-1 during insulin stimulation. *EMBO J. 11*, 3469−3479.
(31) Carpenter, C. L., Auger, K. R., Chanudhuri, M., Yoakim, M., Schaffhausen, B., Shoelson, S., and Cantley, L. C. (1993) Phosphoinositide 3-kinase is activated by phosphopeptides that bind to the SH2 domains of the 85-kDa subunit. *J. Biol. Chem. 268*, 9478−9483.
(32) Samuels, Y., Wang, Z., Bardelli, A., Silliman, N., Ptak, J., Szabo, S., Yan, H., Gazdar, A., Powell, S. M., Riggins, G. J., Willson, J. K., Markowitz, S., Kinzler, K. W., Vogelstein, B., and Velculescu, V. E. (2004) High frequency of mutations of the *PIK3CA* gene in human cancers. *Science 304*, 554.
(33) Ikenoue, T., Kanai, F., Hikiba, Y., Obata, T., Tanaka, Y., Imamura, J., Ohta, M., Jazag, A., Guleng, B., Tateishi, K., Asaoka, Y., Matsumura, M., Kawabe, T., and Omata, M. (2005) Functional analysis of PIK3CA gene mutations in human colorectal cancer. *Cancer Res. 65*, 4562−4567.
(34) Isakoff, S. J., Engelman, J. A., Irie, H. Y., Luo, J., Brachmann, S. M., Pearline, R. V., Cantley, L. C., and Brugge, J. S. (2005) Breast cancer-associated *PIK3CA* mutations are oncogenic in mammary epithelial cells. *Cancer Res. 65*, 10992−11000.
(35) Kang, S., Bader, A. G., and Vogt, P. K. (2005) Phosphatidylinositol 3-kinase mutations identified in human cancer are oncogenic. *Proc. Natl. Acad. Sci. U.S.A. 102*, 802−807.
(36) Ombrello, M. J., Remmers, E. F., Sun, G., Freeman, A. F., Datta, S., Torabi-Parizi, P., Subramanian, N., Bunney, T. D., Baxendale, R. W., Martins, M. S., Romberg, N., Komarow, H., Aksentijevich, I., Kim, H. S., Ho, J., Cruse, G., Jung, M. Y., Gilfillan, A. M., Metcalfe, D. D., Nelson, C., O'Brien, M., Wisch, L., Stone, K., Douek, D. C., Gandhi, C., Wanderer, A. A., Lee, H., Nelson, S. F., Shianna, K. V., Cirulli, E. T., Goldstein, D. B., Long, E. O., Moir, S., Meffre, E., Holland, S. M., Kastner, D. L., Katan, M., Hoffman, H. M., and Milner, J. D. (2012) Cold urticaria, immunodeficiency, and autoimmunity related to *PLCG2* deletions. *N. Engl. J. Med. 366*, 330−338.
(37) Zhou, Q., Lee, G. S., Brady, J., Datta, S., Katan, M., Sheikh, A., Martins, M. S., Bunney, T. D., Santich, B. H., Moir, S., Kuhns, D. B., Long Priel, D. A., Ombrello, A., Stone, D., Ombrello, M. J., Khan, J., Milner, J. D., Kastner, D. L., and Aksentijevich, I. (2012) A hypermorphic missense mutation in PLCG2, encoding phospholipase Cγ2, causes a dominantly inherited autoinflammatory disease with immunodeficiency. *Am. J. Hum. Genet. 91*, 713−720.
(38) Yu, P., Constien, R., Dear, N., Katan, M., Hanke, P., Bunney, T. D., Kunder, S., Quintanilla-Martinez, L., Huffstadt, U., Schroder, A., Jones, N. P., Peters, T., Fuchs, H., de Angelis, M. H., Nehls, M., Grosse, J., Wabnitz, P., Meyer, T. P., Yasuda, K., Schiemann, M., Schneider-Fresenius, C., Jagla, W., Russ, A., Popp, A., Josephs, M., Marquardt, A., Laufs, J., Schmittwolf, C., Wagner, H., Pfeffer, K., and Mudde, G. C. (2005) Autoimmunity and inflammation due to a gain-of-function mutation in phospholipase Cγ2 that specifically increases external Ca^{2+} entry. *Immunity 22*, 451−465.
(39) Everett, K. L., Bunney, T. D., Yoon, Y., Rodrigues-Lima, F., Harris, R., Driscoll, P. C., Abe, K., Fuchs, H., de Angelis, M. H., Yu, P., Cho, W., and Katan, M. (2009) Characterization of phospholipase Cγ enzymes with gain-of-function mutations. *J. Biol. Chem. 284*, 23083−23093.